THE BELL SYSTEM TECHNICAL JOURNAL
Vol. 53, No. 8, October 1974
Printed in U.S.A.

Rain-Induced Cross-Polarization at Centimeter and Millimeter Wavelengths

By T. S. CHU

(Manuscript received March 13, 1974)

Rain-induced cross-polarization is an important factor in design of dual-polarization microwave radio communication systems. We present current estimates of this effect based upon calculated differential characteristics of canted oblate raindrops and their relationship to experiments. Measured differential attenuation and cross-polarization, mainly at 18 GHz, are used to determine two empirical parameters: an effective average of the absolute value of the canting angle and a measure of the imbalance between positive and negative canting angles. We can then provide estimates for median values of cross-polarization discriminations at other frequencies; these are found to agree fairly well with available measured data.

Differential phase shift is the dominant factor in the rain-induced cross-polarization at frequencies below about 10 GHz, and differential attenuation becomes increasingly important at higher frequencies. For a given rain fading, the cross-polarization decreases with increase in frequency and is relatively insensitive to the rain rate, whereas for a given amount of rain the cross-polarization increases with frequency up to about 35 GHz. The cross-polarization discrimination of circularly polarized waves is much poorer than that of linearly polarized waves. When the angle α between the direction of propagation and the axis of symmetry of oblate raindrops is not equal to $\pi/2$, as on earth-space paths in satellite communication systems, the differential attenuation and differential phase shift can be approximated by $\sin^2 \alpha$ times those for $\alpha = \pi/2$, which is the condition for terrestrial paths.

I. INTRODUCTION

Understanding depolarization properties of the transmission medium is of crucial importance in planning frequency reuse by employing orthogonal polarizations in a radio communication system. The rain-induced depolarization, which concurs with heavy rain attenuation,

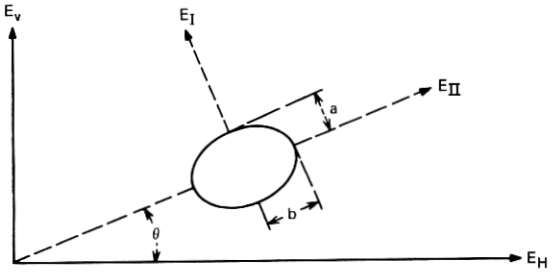

Fig. 1—Canted oblate spheroidal raindrop.

has attracted considerable theoretical and experimental efforts.[1–9] A mathematical model of canted oblate spheroidal raindrops as shown in Fig. 1 has been assumed in most theoretical investigations. Cross-coupling between vertical and horizontal polarizations occurs as a result of the differential attenuation and differential phase shift between two polarizations parallel and perpendicular to a major axis of the oblate raindrops. Recently, Morrison et al.[10,11] have given the calculated differential characteristics for various rain rates throughout the microwave range from 4 to 100 GHz. These results are based upon numerical solutions[12] of the scattering of a plane electromagnetic wave by oblate spheroidal raindrops using a point-matching procedure or perturbation about an equivolumic sphere. The modified perturbation scheme[11] offers a substantial improvement over Oguchi's previous perturbation calculations.[1] Very recently, Oguchi[13,14] also used a point-matching procedure to make similar calculations. The purpose of this paper is to assess our current understanding of the rain-induced microwave depolarization in view of these new calculations and their relationship to the measured data.

Table I — Attenuation and phase shift at 4 GHz with $\alpha = 90°$

Rain Rate in mm/hr	A_I in dB/km	A_{II} in dB/km	Φ_I in deg/km	Φ_{II} in deg/km
0.25	1.825×10^{-4}	2.013×10^{-4}	1.413×10^{-1}	1.487×10^{-1}
1.25	7.806×10^{-4}	8.931×10^{-4}	5.494×10^{-1}	5.894×10^{-1}
2.5	1.506×10^{-3}	1.759×10^{-3}	9.933×10^{-1}	1.077
5.0	2.980×10^{-3}	3.570×10^{-3}	1.806	1.984
12.5	7.581×10^{-3}	9.435×10^{-3}	3.995	4.478
25.0	1.610×10^{-2}	2.089×10^{-2}	7.377	8.417
50.0	3.547×10^{-2}	4.836×10^{-2}	13.83	16.10
100.0	8.038×10^{-2}	1.164×10^{-1}	26.15	31.10
150.0	1.324×10^{-1}	2.021×10^{-1}	38.35	46.23

Table II — Attenuation and phase shift at 11 GHz with $\alpha = 90°$

Rain Rate in mm/hr	A_I in dB/km	A_{II} in dB/km	Φ_I in deg/km	Φ_{II} in deg/km
0.25	2.428×10^{-3}	2.669×10^{-3}	3.985×10^{-1}	4.195×10^{-1}
1.25	1.592×10^{-2}	1.820×10^{-2}	1.579	1.697
2.5	3.787×10^{-2}	4.399×10^{-2}	2.880	3.127
5.0	9.144×10^{-2}	1.076×10^{-1}	5.266	5.783
12.5	2.907×10^{-1}	3.470×10^{-1}	11.69	13.06
25.0	6.898×10^{-1}	8.293×10^{-1}	21.32	24.18
50.0	1.605	1.945	38.94	44.93
100.0	3.586	4.392	70.25	82.58
150.0	5.605	6.919	99.26	118.3

The considerable uncertainty about the canting-angle distribution can be characterized by two parameters as suggested by Thomas.[2] The first parameter, which is an effective average of the absolute value of the canting angle, can be determined by comparing the calculated values with the measured differential attenuation between vertical and horizontal polarizations. The second parameter, which is a measure of the imbalance between positive and negative canting angles with respect to the vertical direction, can be determined by comparison between the calculated and measured cross-polarizations. The reliability of empirical parameters will be much improved by recent developments in theory and experiment. Then the theoretical model provides systematic extrapolation of the measured data.

Section II tabulates the details of the calculated attenuation and phase shift that were abbreviated in Ref. 10. The normalized differential characteristics with respect to rain fading give physical insight and the main features of the rain-induced cross-polarization. Section III describes the calculation of depolarization for both linearly and

Table III — Attenuation and phase shift at 18.1 GHz with $\alpha = 90°$

Rain Rate in mm/hr	A_I in dB/km	A_{II} in dB/km	Φ_I in deg/km	Φ_{II} in deg/km
0.25	9.797×10^{-3}	1.071×10^{-2}	6.674×10^{-1}	7.029×10^{-1}
1.25	6.483×10^{-2}	7.275×10^{-2}	2.608	2.801
2.5	1.458×10^{-1}	1.658×10^{-1}	4.680	5.078
5.0	3.205×10^{-1}	3.702×10^{-1}	8.362	9.182
12.5	8.927×10^{-1}	1.055	17.78	19.90
25.0	1.874	2.273	31.33	35.63
50.0	3.869	4.846	55.24	63.88
100.0	7.696	10.04	97.39	114.1
150.0	11.5	15.39	137.0	161.4

Table IV — Attenuation and phase shift at 30 GHz with $\alpha = 90°$

Rain Rate in mm/hr	A_I in dB/km	A_{II} in dB/km	Φ_I in deg/km	Φ_{II} in deg/km
0.25	3.347×10^{-2}	3.660×10^{-2}	1.102	1.160
1.25	1.960×10^{-1}	2.221×10^{-1}	4.134	4.428
2.5	4.121×10^{-1}	4.757×10^{-1}	7.220	7.789
5.0	8.506×10^{-1}	1.001	12.51	13.57
12.5	2.179	2.634	25.26	27.56
25.0	4.321	5.321	42.54	46.31
50.0	8.444	10.58	71.16	76.72
100.0	15.96	20.25	118.6	125.2
150.0	23.05	29.37	161.3	167.7

circularly polarized waves. Section IV determines empirical parameters of the canting-angle distribution. Estimates are made for the median values of the rain-induced depolarization at centimeter and millimeter wavelengths. An approximation for the case of oblique propagation is also examined.

II. DIFFERENTIAL ATTENUATION AND DIFFERENTIAL PHASE SHIFT

The ratio of minor to major axes of the oblate spheroidal raindrop is assumed to be linearly dependent upon the radius $\bar{a}$ (in centimeters) of the equivolumic spherical drop; specifically, $a/b = 1 - \bar{a}$. This relationship is a simple approximation for the experimental data of the drop shape.[15] Morrison and Cross[12] have used a least-squares-fitting procedure to calculate the complex forward scattering functions $S_I(0)$ and $S_{II}(0)$[16] for the two polarizations I and II parallel and perpendicular to the plane containing the axis of symmetry of the raindrop and the direction of propagation of the incident wave. They have given numerical tables of forward scattering functions for all the raindrop sizes

Table V — Attenuation and phase shift at 30 GHz with $\alpha = 70°$

Rain Rate in mm/hr	A_I in dB/km	A_{II} in dB/km	Φ_I in deg/km	Φ_{II} in deg/km
0.25	3.372×10^{-2}	3.648×10^{-2}	1.108	1.160
1.25	1.984×10^{-1}	2.215×10^{-1}	4.170	4.433
2.5	4.183×10^{-1}	4.746×10^{-1}	7.293	7.803
5.0	8.664×10^{-1}	9.996×10^{-1}	12.66	13.61
12.5	2.230	2.633	25.61	27.67
25.0	4.440	5.326	43.18	46.53
50.0	8.712	10.60	72.26	77.19
100.0	16.53	20.33	120.3	126.1
150.0	23.91	29.50	163.4	168.9

Table VI — Attenuation and phase shift at 30 GHz with $\alpha = 50°$

Rain Rate in mm/hr	A_I in dB/km	A_{II} in dB/km	Φ_I in deg/km	Φ_{II} in deg/km
0.25	3.433×10^{-2}	3.617×10^{-2}	1.127	1.161
1.25	2.045×10^{-1}	2.199×10^{-1}	4.272	4.447
2.5	4.343×10^{-1}	4.719×10^{-1}	7.501	7.840
5.0	9.068×10^{-1}	9.959×10^{-1}	13.07	13.70
12.5	2.362	2.632	26.57	27.93
25.0	4.746	5.339	44.90	47.11
50.0	9.398	10.67	75.17	78.36
100.0	17.97	20.52	124.7	128.3
150.0	26.10	29.84	168.8	172.0

of the Laws and Parsons distribution. The rain-induced attenuation and phase shift are obtained from the forward scattering functions as[16]

$$A_{I,II} = 0.434 \frac{\lambda^2}{\pi} \sum \operatorname{Re} S_{I,II}(0) n(\bar{a}) \qquad \text{(dB/km)} \qquad (1)$$

$$\phi_{I,II} = -36 \frac{\lambda^2}{4\pi^2} \sum \operatorname{Im} S_{I,II}(0) n(\bar{a}) \qquad \text{(deg/km)}, \qquad (2)$$

where λ is the wavelength in centimeters and $n(\bar{a})$ is the number of drops with equivolumic radius $\bar{a}$ per cubic meter. For $\alpha = 90°$, the attenuation and phase shift for various rain rates at 4, 11, 18.1, and 30 GHz have been listed in Tables I to IV. Here α is the angle between the direction of propagation and the axis of symmetry of the raindrop. The

Table VII — Index of refraction of water at 20°C (computed from a recent empirical equation in Ref. 17)

Frequency in GHz	Index of Refraction
4	$8.77 + 0.915i$*
5	$8.685 + 1.195i$
6	$8.574 + 1.399i$
8	$8.319 + 1.761i$
11	$7.884 + 2.184i$
14	$7.437 + 2.477i$
18.1	$6.859 + 2.716i$
20	$6.614 + 2.780i$
24	$6.151 + 2.849i$
30	$5.581 + 2.848i$
40	$4.886 + 2.725i$
60	$4.052 + 2.393i$
100	$3.282 + 1.864i$

* Since the calculations at 4 GHz were made at an earlier date, the 4-GHz refractive index was taken from the older literature (Ref. 18).

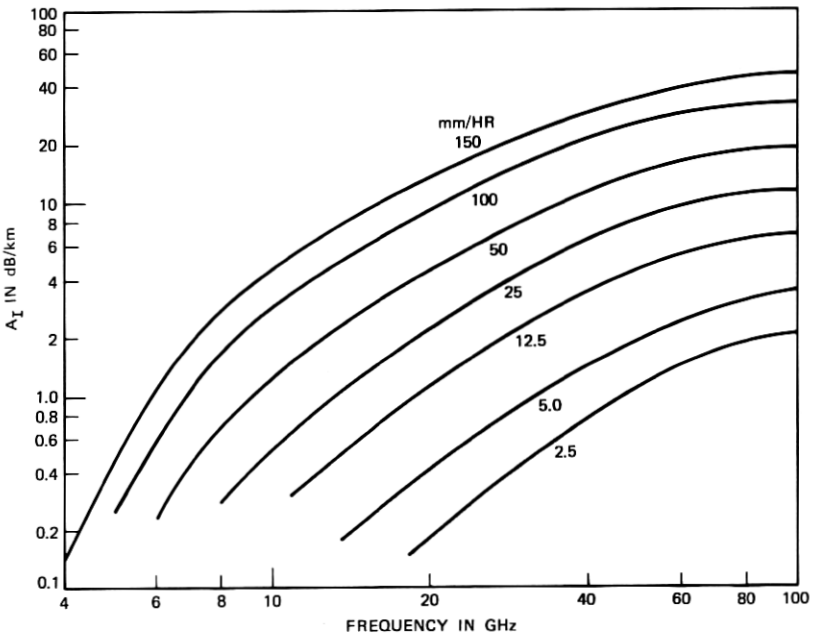

Fig. 2—Calculated attenuation coefficients of polarization I from perturbation about an equivolumic sphere.

cases $\alpha = 50°$ and $70°$ at 30 GHz have been listed in Tables V and VI. The differential attenuation and the differential phase shift were presented graphically in Ref. 10, whereas the above tables are documented here for the reader interested in more details. Most results of this paper belong to the case $\alpha = 90°$, which is pertinent to terrestrial microwave relay systems. However, we discuss later an approximation for other values of α that are of interest in satellite systems.

Since the results of a modified perturbation scheme showed close agreement with those of the least-squares-fitting procedure, the rain-induced differential attenuation and differential phase shift based upon that perturbation scheme have been graphically presented[11] for various rain rates from 4 to 100 GHz. As a supplement to Ref. 11, the refractive indices used for the calculations are listed in Table VII, computed from an equation in Ref. 17. For a given rain rate, the differential attenuation increases with frequency until about 35 GHz, whereas the differential phase shift peaks around 20 GHz and then decreases sharply to negative values for millimeter wavelengths. The

cross-polarization is expected to increase with frequency until about 35 GHz for a given amount of rain.

As reference, Fig. 2 presents A_I obtained from the modified perturbation scheme. Combining Fig. 2 with the differential attenuation data of Ref. 11 results in A_{II}. In comparison with Setzer's data,[18] we note that the attenuation by equivolumic spherical drops lies between A_I and A_{II}, but closer to A_{II}. Since the average of the absolute value of the canting angle is about 25°, as demonstrated later, the attenuation of vertical polarization will be greater than A_I, whereas the attenuation of horizontal polarization will be less than A_{II}.

A communication system is usually designed for a certain margin of fading. In propagation experiments, attenuation and cross-polarization

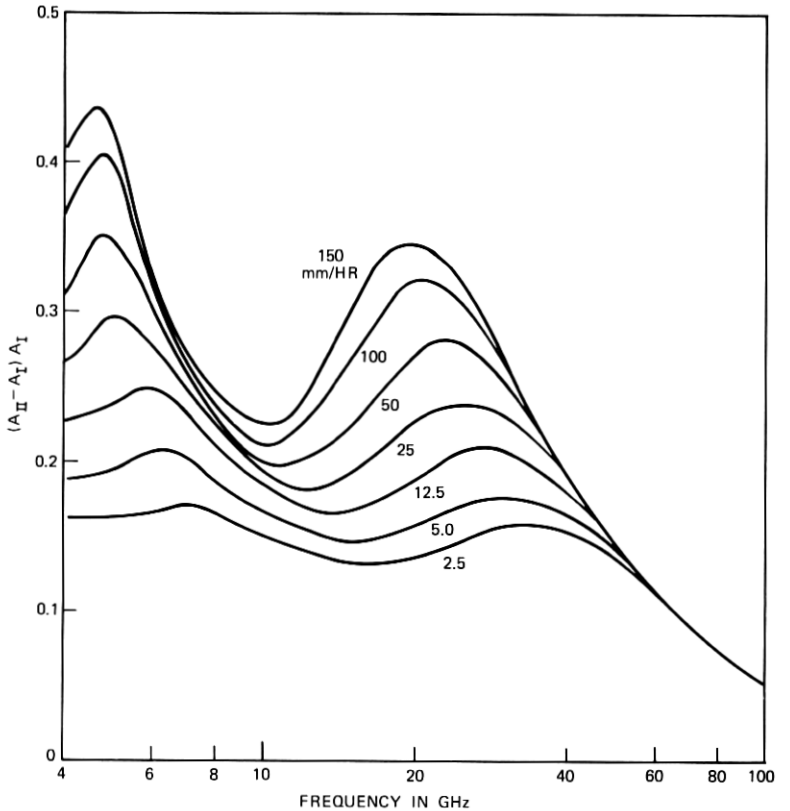

Fig. 3—Normalized differential attenuation with respect to A_I.

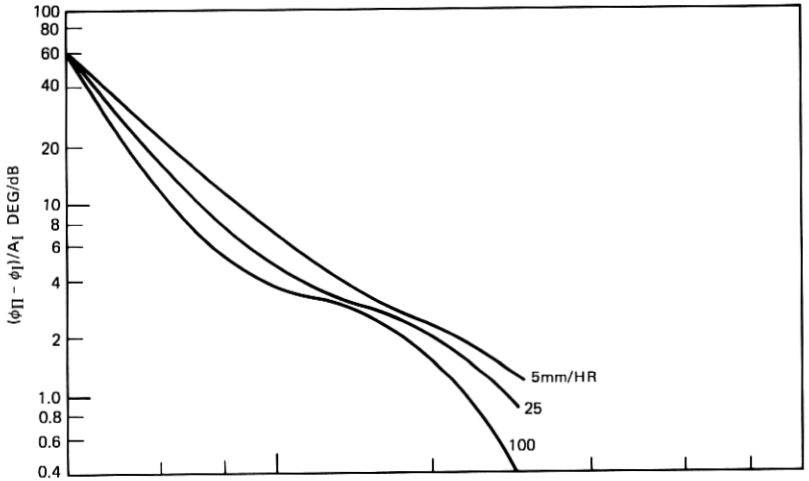

Fig. 4a—Normalized differential phase shift with respect to A_I (4 to 30 GHz).

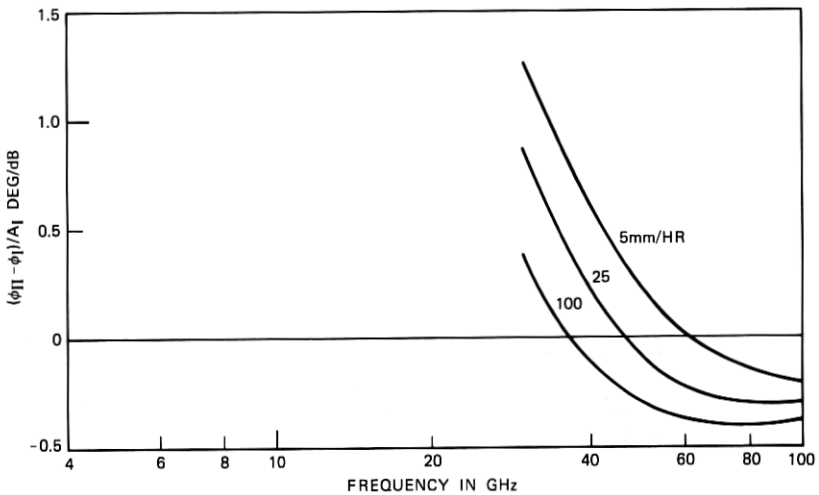

Fig. 4b—Normalized differential phase shift with respect to A_I (30 to 100 GHz).

are often simultaneously measured for correlation with each other. The above two considerations suggest the normalization of both differential attenuation and differential phase shift with respect to the attenuation of polarization I as shown in Figs. 3, 4a, and 4b. These presentations invite a number of observations, as described below.

It is well known that the rain attenuation of longer microwaves such as 4 GHz is slight. Therefore, the relatively high ratio for the nor-

malized differential attenuation in this frequency region will make little contribution to depolarization. However, the very high differential phase shift at 4 GHz in Fig. 4a indicates that significant depolarization is possible even for only a few decibels of attenuation that can occur on a long path, say 40 km between two repeaters. Barnett[8] has reported experimental observations of 4-GHz depolarization during heavy rain. Here, the differential phase shift is indeed the dominant cause of rain-induced depolarization.

For a given fade, the differential phase shift declines sharply with the increase in frequency, whereas the normalized differential attenuation is relatively insensitive to frequency. Therefore, the differential attenuation becomes increasingly important as the frequency increases. The differential attenuation in nepers and the differential phase shift in radians are about the same at about 20 GHz. The sharp descent of the differential phase shift also implies less depolarization at higher microwave frequencies for a given fade.

We note that the decline of the differential phase shift continues into negative values at millimeter wavelengths as shown in Fig. 4b. Although the absolute accuracy of the differential phase shift above 30 GHz is somewhat doubtful in view of its dependence on the cancellation between large numbers, we should expect small differential phase shift per decibel of fading at millimeter wavelengths. Furthermore, the normalized differential attenuation also becomes small because smaller rain drops of less ellipticity are contributing heavily to the attenuation at shorter wavelengths. Delange et al.[19] observed only 2-dB differential attenuation between vertical and horizontal polarizations with a rain fading of 40 dB at 60 GHz.

As the rain rate decreases, the normalized differential attenuation of each frequency decreases. On the other hand, the differential phase shift per decibel of fading generally increases with the decrease of the rain rate. These two opposite trends tend to keep the depolarization relatively insensitive to the rain rate, as is shown in Section 4.2.

III. CALCULATION OF DEPOLARIZATION

Let the axis of symmetry of the oblate raindrop be oriented with respect to the vertical direction at an angle θ, called the canting angle, which is discussed later. We now calculate the depolarization resulting from the anisotropy described in the preceding section. In practice, dual-polarization radio communication systems employ either two orthogonal linear or circular polarizations. The orthogonal linear polarizations are usually aligned in the vertical and horizontal direc-

tions. The polarization transformation of an anisotropic medium can be conveniently obtained by listing the following matrix operations:

$$\begin{pmatrix} H_0 \\ V_0 \end{pmatrix} = \begin{pmatrix} \cos\theta & -\sin\theta \\ \sin\theta & \cos\theta \end{pmatrix} \begin{pmatrix} T_2 & 0 \\ 0 & T_1 \end{pmatrix} \begin{pmatrix} \cos\theta & \sin\theta \\ -\sin\theta & \cos\theta \end{pmatrix} \begin{pmatrix} H_i \\ V_i \end{pmatrix}, \tag{3}$$

where T_2 and T_1 are the transmission coefficients over a path of length L for polarizations II and I,

$$T_2 = \exp\,[-\,(\alpha_2 - j\beta_2)L], \tag{4}$$

$$T_1 = \exp\,[-\,(\alpha_1 - j\beta_1)L]. \tag{5}$$

Carrying out the multiplication of the matrices yields the relationship between input (transmitted) and output (received) polarizations:

$$\begin{pmatrix} H_0 \\ V_0 \end{pmatrix} = \begin{pmatrix} a_{hh} & a_{hv} \\ a_{vh} & a_{vv} \end{pmatrix} \begin{pmatrix} H_i \\ V_i \end{pmatrix}, \tag{6}$$

where

$$a_{hh} = T_2 \cos^2\theta + T_1 \sin^2\theta, \tag{7}$$

$$a_{vv} = T_1 \cos^2\theta + T_2 \sin^2\theta, \tag{8}$$

$$a_{hv} = a_{vh} = \left(\frac{T_2 - T_1}{2}\right) \sin 2\theta. \tag{9}$$

The following expressions are given for the convenience of computation:

$$|a_{hh}|^2 = \exp\,[-\,(\alpha_1 + \alpha_2)L](D + C\cos^2 2\theta - E\cos 2\theta), \tag{10}$$

$$|a_{vv}|^2 = \exp\,[-\,(\alpha_1 + \alpha_2)L](D + C\cos^2 2\theta + E\cos 2\theta), \tag{11}$$

$$|a_{hv}|^2 = \exp\,[-\,(\alpha_1 + \alpha_2)L]\; C\sin^2 2\theta, \tag{12}$$

where

$$C = \cos^2\beta L \sinh^2\alpha L + \sin^2\beta L \cosh^2\alpha L, \tag{13}$$

$$D = \cosh^2\alpha L \cos^2\beta L + \sinh^2\alpha L \sin^2\beta L, \tag{14}$$

$$E = 2\cosh\alpha L \sinh\alpha L. \tag{15}$$

The differential attenuation coefficient and the differential phase shift coefficient are $2\alpha = \alpha_2 - \alpha_1$ and $2\beta = \beta_2 - \beta_1$, respectively. When αL (in nepers) and βL (in radians) are small, eq. (13) may be approximated by $C = (\alpha L)^2 + (\beta L)^2$.

Since both a_{hh} and a_{vv} are independent of the sign of θ, an average of the absolute value of the canting angle can be obtained by comparing the calculated $|a_{hh}/a_{vv}|$ for various θ with the measured differential attenuation between vertical and horizontal polarizations. The ex-

pressions for $a_{hv} = a_{vh}$ indicate that the cross-polarized components resulting from positive and negative canting angles tend to cancel each other. Furthermore, Saunders[9] found from photographs of falling raindrops that the canting angle is not far from an even distribution between the positive and the negative senses. Then the cross-polarization coefficient $|a_{hv}|$ or $|a_{vh}|$ should be reduced by a factor ϵ which is a measure of the imbalance between positive and negative canting angles. Having first obtained the average of the absolute value of the canting angle, ϵ can be determined by comparison between the calculated and measured cross-polarization data.

Then, when transmitting horizontal and vertical polarizations the crosstalk discriminations are

$$\text{XTDH} = \epsilon^2 \left| \frac{a_{hv}}{a_{hh}} \right|^2 = \frac{\epsilon^2 C \sin^2 2\theta}{D + C \cos^2 2\theta - E \cos 2\theta} \tag{16a}$$

for receiving horizontal polarization, and

$$\text{XTDV} = \epsilon^2 \left| \frac{a_{vh}}{a_{vv}} \right|^2 = \frac{\epsilon^2 C \sin^2 2\theta}{D + C \cos^2 2\theta + E \cos 2\theta} \tag{16b}$$

for receiving vertical polarization. The crosstalk discriminations are important information for communication systems. In propagation experiments, we often receive both horizontal and vertical polarizations with one transmitted polarization. The cross-polarization discriminations are

$$\text{XPDH} = \epsilon^2 \left| \frac{a_{vh}}{a_{hh}} \right|^2 = \frac{\epsilon^2 C \sin^2 2\theta}{D + C \cos^2 2\theta - E \cos 2\theta} \tag{17a}$$

for transmitting horizontal polarization and

$$\text{XPDV} = \epsilon^2 \left| \frac{a_{hv}}{a_{vv}} \right|^2 = \frac{\epsilon^2 C \sin^2 2\theta}{D + C \cos^2 2\theta + E \cos 2\theta} \tag{17b}$$

for transmitting vertical polarization. The crosstalk discriminations in (16) are numerically the same as the cross-polarization discriminations in (17). Experimental confirmation of this theoretical equivalence based on the simple model has been reported by Watson and Arbabi.[20]

The attenuation is greater in horizontal than in vertical polarization because the effective average of the absolute value of raindrop canting angle is estimated to be about 25°, as shown in the next section. Then XPDH will be poorer than XPDV. Since $a_{hv} = a_{vh}$, the difference between XPDH and XPDV for the same rain is expected to be the

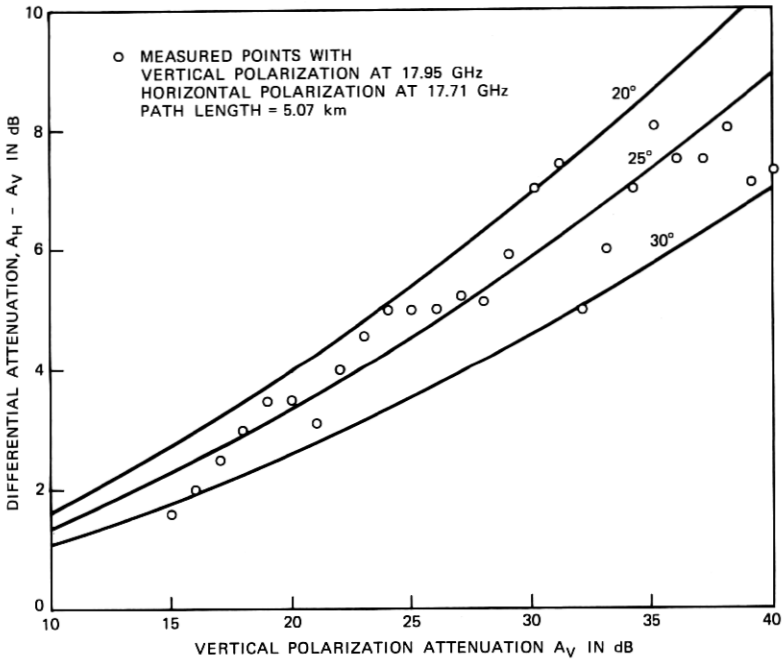

Fig. 5—Comparison between calculated and measured differential attenuation at 18 GHz.

same as the differential attenuation between horizontal and vertical polarizations.

Now let us examine the case of circular polarization. The polarization ratio V/H is first obtained from the following transformation:

$$\begin{pmatrix} \mathrm{H} \\ \mathrm{V} \end{pmatrix} = \begin{pmatrix} a_{hh} & a_{hv} \\ a_{vh} & a_{vv} \end{pmatrix} \begin{pmatrix} 1 \\ j \end{pmatrix}. \tag{18}$$

The ratio of the desired circular polarization to the undesired rain-induced circular polarization is[21]

$$\frac{1 - j\mathrm{V/H}}{1 + j\mathrm{V/H}} = \frac{T_2 + T_1}{T_2 - T_1} e^{-j2\theta}. \tag{19}$$

The cross-polarization discrimination of circular polarization becomes

$$\mathrm{XPDC} = \left| \frac{T_2 - T_1}{T_2 + T_1} \overline{e^{j2\theta}} \right|^2 = (|a_{vh}/a_{hh}|^2_{\theta=45°}) |\overline{e^{j2\theta}}|^2, \tag{20}$$

where the mean value of $e^{j2\theta}$ is taken over the canting angle distribu-

tion. If all the oblate raindrops are oriented at a single canting angle, XPDC is equal to $|a_{vh}/a_{hh}|^2$ with $\theta = 45°$. In view of the uncertainty of the canting angle distribution, comparison between the measured and calculated cross-polarizations will be used to estimate this reduction factor $|\overline{e^{j2\theta}}|^2$. We also note that the cross-polarization discriminations of two circular polarizations should be equal to each other.

IV. NUMERICAL RESULTS AND DISCUSSIONS

4.1 XPD of vertical and horizontal polarizations

We first estimate an effective average of the absolute value of the canting angle by comparing the calculated differential attenuation with the measured data. Such comparisons are shown in Figs. 5 and 6 for 18 and 30 GHz. The calculated curves assume that the canting

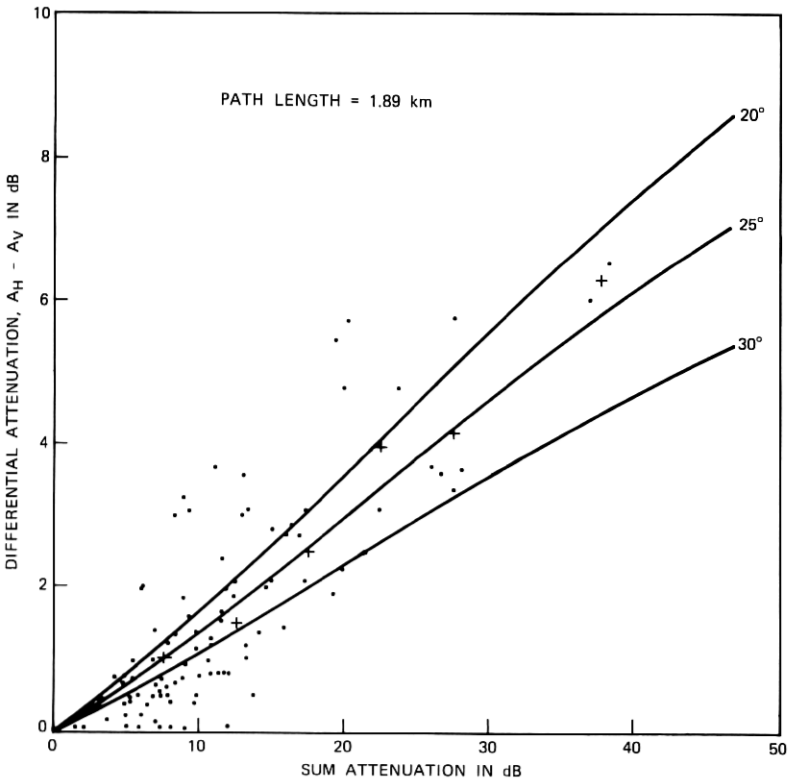

Fig. 6—Comparison between calculated and measured differential attenuation at 30 GHz.

angles of all raindrops are oriented at 20°, 25°, and 30° from the vertical direction. A uniform rain rate has been also imposed over each measured path in the calculations.

The 18-GHz data in Fig. 5 are obtained by W. T. Barnett[7] and S. H. Lin[22] in Georgia. R. A. Semplak's 30-GHz measurement[5] in New Jersey is shown in Fig. 6, where the dots indicate the scatter of the original data and the crosses are median values at 5-dB intervals. The abscissa in Fig. 5 is simply the attenuation of vertically polarized waves, whereas the one in Fig. 6 is the sum attenuation, $\frac{1}{2}(|a_{hh}|^2 + |a_{vv}|^2)$, which represents the received power sum of the horizontal and vertical components of a transmitted wave linearly polarized at 45° from the vertical direction. It is evident from the comparisons in Figs. 5 and 6 that 25° is a good estimate for an effective average of the absolute value of the canting angle. Substituting $|\theta| = 25°$ in (10) and (11) yields the calculated attenuation of vertically and horizontally polarized waves as shown in Fig. 7. We note that an effective average of the

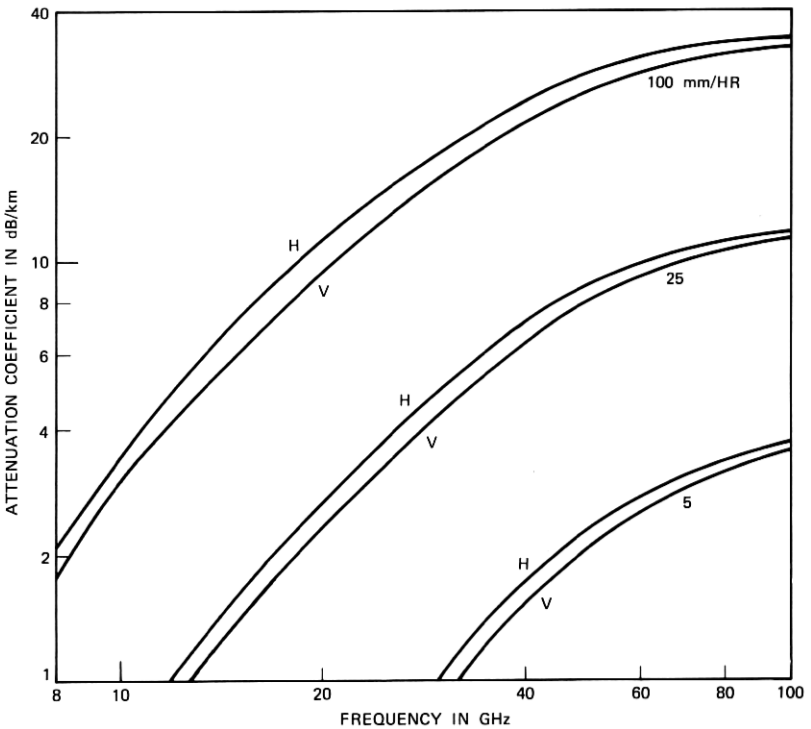

Fig. 7—Attenuation coefficients of vertically and horizontally polarized waves.

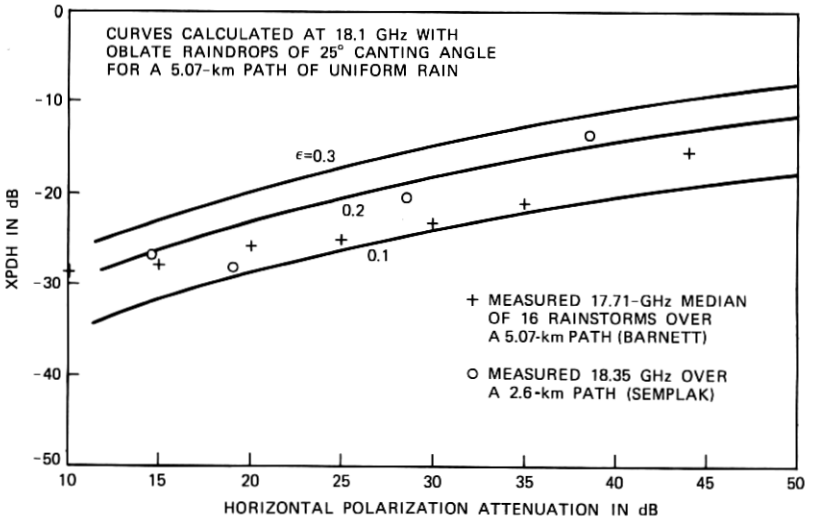

Fig. 8—Comparison between calculated and measured cross-polarization discriminations at 18 GHz.

absolute value of the canting angle should not be mistaken for the mean canting angle,[23] which is much smaller.*

Next, an estimate is made of the imbalance between positive and negative canting angles by comparing the calculated cross-polarization discrimination with the measured data. The calculated curves in Figs. 8 and 9 are computed from (17) with $|\theta| = 25°$ and ϵ assumed as 0.1, 0.2, and 0.3. Uniform rain rates have been assumed over the propagation path in the calculations. The crosses in Fig. 8 are Barnett's measured 17.71-GHz median XPDH of 16 rain storms in Georgia.[7,21] The dots from Semplak's 18.35-GHz measurements[24] over a 2.6-km path are given in Fig. 8 to provide a check. The measured XPDV points in Fig. 9 are deduced from polarization rotation measurements[25] at 30.9 GHz, where the effect of the differential phase shift has been assumed to be negligible. The assumption is approximately valid at this frequency for heavy rain. Figures 8 and 9 show that the measured data are largely confined within the curves with $\epsilon = 0.1$ and 0.2, and hence suggest the geometric mean 0.14 as a good estimate for the median value of ϵ.

Having determined the parameters $|\theta| = 25°$ and $\epsilon = 0.14$, we can use (16) to calculate crosstalk ratios vs attenuation of transmitted

* If the canting angle distribution is simulated by a gaussian model, then the mean will be 2 to 3° and the standard deviation will be 30 to 40°.

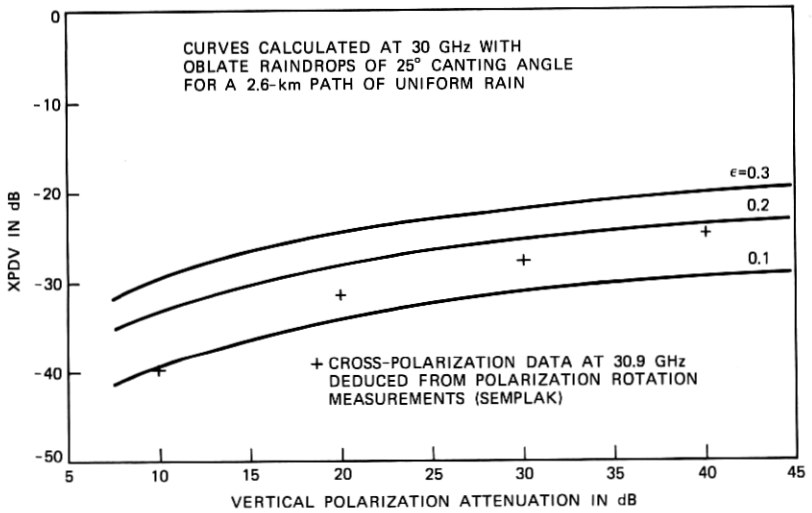

Fig. 9—Comparison between calculated and measured cross-polarization discriminations at 30 GHz.

signal for various frequencies at 100 mm/hr rain rate, as shown in Fig. 10. The solid and dashed curves are expected to be median values at 100 mm/hr rain rate for XPDH and XPDV, respectively. For a given rain fading, the cross-polarization increases with decreasing frequency. However, 4- and 6-GHz communication systems seldom experience rain attenuation of more than a few decibels. Although it takes a slightly heavier rain for the vertically polarized signal to suffer the same fading as the horizontally polarized signal, XPDV is generally less than XPDH for the same fading, except at lower frequencies such as 4 GHz, where the differential phase shift dominates the cross-polarization excitation.

In addition to explaining the measured cross-polarization at 18 and 30 GHz, the predicted cross-polarization discriminations in Fig. 10 also agree fairly well with measured data at 4 GHz of Barnett,[8] at 11 GHz of Watson and Arbabi[26] and Evans and Thompson,[27] at 20 GHz of Yamamoto et al.,[28] and at 60 GHz of Delange et al.[19] The lack of precise agreement stems not only from the imperfection of the theoretical model but also from the measuring error of the experiments. Ground reflection and antenna depolarization often limit the cross-polarization discrimination of measuring systems to around −35 dB in clear weather.

Measurements show considerable variance of cross-polarization discrimination at a given rain attenuation. This factor must be kept in mind when median values of cross-polarization discriminations at given rain fades are used for the design of a dual-polarization radio communication system. The worst cross-polarization discrimination can be 5 to 10 dB above the median values, whereas it is also possible to have very little cross-polarization when almost perfect cancellation occurs among the raindrop canting-angle distribution, i.e., $\epsilon \rightarrow 0$. For more precise predictions of radio channel reliability, the joint statistics of rain fading and cross-polarization discrimination should be considered.

4.2 Effect of rain rate

Measured statistics will always be needed for the design of communication systems. In order to extrapolate statistical results from

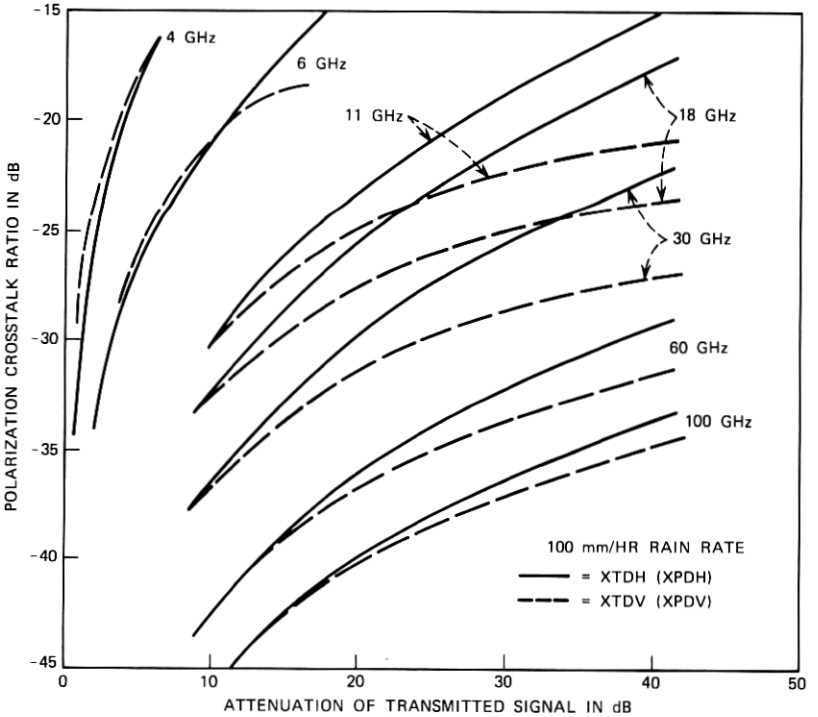

Fig. 10—Calculated rain-induced cross-polarization of horizontally and vertically polarized waves.

one measured path to another path of different length, it is essential to know the effect of rain rate on depolarization for a given fading. Qualitative discussions in Section II already suggest that the depolarization is relatively insensitive to rain rate. This observation is now confirmed in Fig. 11, where XPDH versus frequency are plotted for 20-dB fading at three rain rates of 100, 25, and 5 mm/hr.

4.3 XPD of circular polarization

Equation (20) has been used to calculate the rain-induced cross-polarization of circularly polarized waves as shown in Fig. 12. To obtain agreement between the calculated curves and the measured median values of Semplak[6] at 18 GHz, the canting-angle reduction factor $|\overline{e^{j2\theta}}|^2$ has been empirically determined as 8 dB. On the other hand, Saunders' measured canting-angle distribution yields a reduction factor of 6 dB. In view of the variability of the rain storm, the above discrepancy does not seem unreasonable. Comparison of Figs. 10 and 12 shows that the rain-induced depolarization of circularly

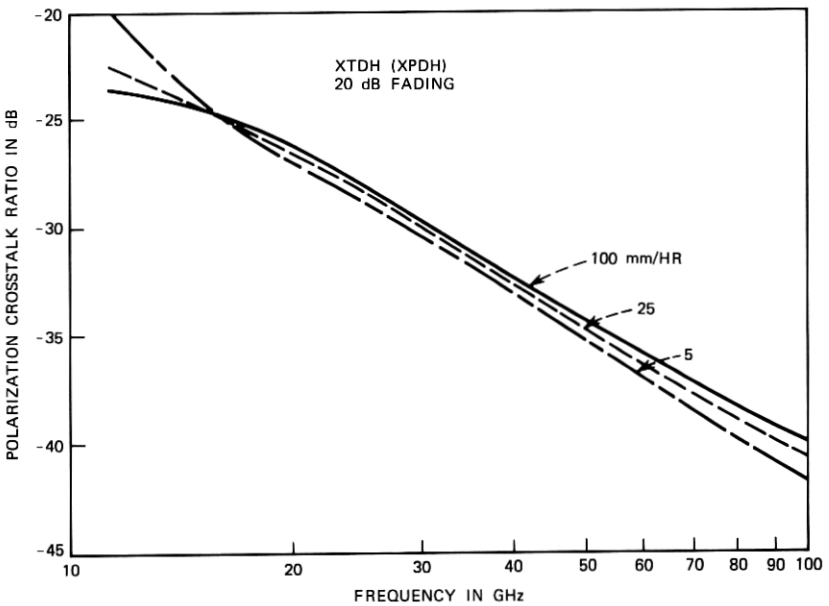

Fig. 11—Cross-polarization at 20-dB fading for various rain rates.

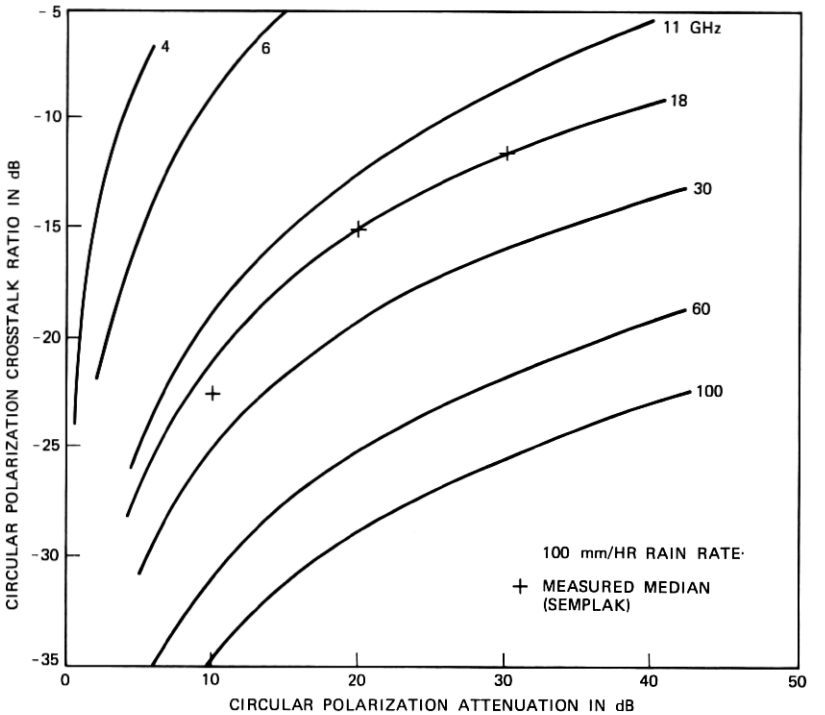

Fig. 12—Calculated rain-induced cross-polarization of circularly polarized waves.

polarized waves is about 10 dB worse than that of a horizontally polarized wave.*

4.4 Oblique propagation

The above numerical results have been confined to the case of $\alpha = \pi/2$, where α is the angle between the direction of propagation and the axis of symmetry of oblate raindrops. This case corresponds to terrestrial microwave relay systems, whereas other values of α are of interest in satellite systems. Limited data for the latter cases are also available from point-matching scattering solutions.[10,14] However, the following approximate relations exist:

$$(A_{II} - A_I)_\alpha = (A_{II} - A_I)_{\pi/2} \sin^2 \alpha, \tag{21}$$

$$(\Phi_{II} - \Phi_I)_\alpha = (\Phi_{II} - \Phi_I)_{\pi/2} \sin^2 \alpha. \tag{22}$$

* The depolarization of a signal linearly polarized at 45° from vertical is expected to be about the same as that of a circularly polarized wave (Ref. 29).

Table VIII — 30-GHz differential attenuation in dB/km

p in mm/hr	$\alpha = 90°$	$\alpha = 70°$	$\alpha = 50°$
0.25	0.00313	0.00276(0.00276)*	0.00184(0.00184)
1.25	0.0261	0.0231(0.0230)	0.0154(0.0153)
2.5	0.0637	0.0563(0.0562)	0.0376(0.0374)
5.0	0.150	0.133(0.133)	0.0890(0.0886)
12.5	0.455	0.403(0.402)	0.270(0.267)
25.0	1.00	0.886(0.883)	0.593(0.587)
50.0	2.14	1.89(1.89)	1.27(1.26)
100.0	4.29	3.80(3.79)	2.54(2.52)
150.0	6.32	5.60(5.58)	3.74(3.71)

* Numbers in parentheses are $\Delta A_{\alpha=90°} \sin^2 \alpha$.

The above approximation was also suggested by Evans and Troughton.[30] A simple derivation in the appendix illustrates the underlying assumption. This low-frequency approximation has been tested by comparison with 30-GHz point-matching results of $\alpha = 70°$ and $\alpha = 50°$.[10] Tables VIII and IX show excellent agreement except for the differential phase shift of heavy rain rates at $\alpha = 50°$, where cancellation between large numbers is involved.

Making use of eqs. (21) and (22), we can predict the cross-polarization discriminations of satellite systems by simply dividing the abscissa scale by $\sin^2 \alpha$ in Fig. 10. Here, the incident linear polarization from the satellite has been assumed to be parallel or orthogonal to the plane containing the direction of propagation and the local gravity direction of the ground station. When this assumption is violated in the fringe area of an area coverage satellite antenna, higher cross-polarization is expected.

Table IX — 30-GHz differential phase shift in deg/km

p in mm/hr	$\alpha = 90°$	$\alpha = 70°$	$\alpha = 50°$
0.25	0.0585	0.0521(0.0517)*	0.0346(0.0343)
1.25	0.294	0.263(0.260)	0.175(0.173)
2.5	0.569	0.510(0.502)	0.339(0.334)
5.0	1.06	0.952(0.936)	0.632(0.622)
12.5	2.30	2.06(2.03)	1.36(1.35)
25.0	3.77	3.36(3.33)	2.21(2.21)
50.0	5.56	4.93(4.91)	3.20(3.26)
100.0	6.59	5.77(5.82)	3.59(3.87)
150.0	6.43	5.53(5.68)	3.23(3.77)

* Numbers in parentheses are $\Delta\phi_{\alpha=90°} \sin^2 \alpha$.

V. ACKNOWLEDGMENT

This paper is built upon the basic work of J. A. Morrison and M.-J. Cross.[12] The author is indebted to J. A. Morrison, D. C. Hogg, and M. J. Gans for helpful discussions, and to D. Vitello for assistance with the computation. He also wishes to thank W. Y. S. Chen and R. P. Slade for reviewing the manuscript.

APPENDIX

Approximation for Oblique Propagation

If the axis of symmetry of each oblate spheroidal raindrop is aligned in the same direction and the raindrop radius is small compared with wavelength, then a uniform rain can be approximately characterized as an anisotropic medium with the relative dielectric constant given in the Cartesian coordinates (XYZ):

$$\bar{\bar{\epsilon}} = \begin{pmatrix} \epsilon_1 & 0 & 0 \\ 0 & \epsilon_2 & 0 \\ 0 & 0 & \epsilon_2 \end{pmatrix} = \begin{pmatrix} n_1^2 & 0 & 0 \\ 0 & n_2^2 & 0 \\ 0 & 0 & n_2^2 \end{pmatrix}. \tag{23}$$

The governing equation for a plane wave $e^{\bar{\gamma}\cdot\bar{r}}$ is simply

$$\bar{\gamma} \times (\bar{\gamma} \times \bar{E}) = k^2 \bar{\bar{\epsilon}} \cdot \bar{E}. \tag{24}$$

In view of the symmetrical property of the medium, the arbitrary direction of propagation, $\bar{\gamma}$, may be confined to the XZ-plane without loss of generality. Let the angle between the direction of propagation and the axis of symmetry (x-axis) be denoted by α. Now we consider two polarizations with subscripts I and II designating the electric fields parallel and perpendicular to the plane containing the axis of symmetry and the direction of propagation. Polarization II has only one electric field component, E_y. Substituting $\bar{E} = E_y\hat{y}$ into (24) immediately yields

$$\gamma_{\text{II}}^2 = -k^2 n_2^2. \tag{25}$$

Polarization I has two electric field components, E_x and E_y. Substituting them into eq. (24) gives two equations:

$$(k^2 n_1^2 + \gamma_{\text{I}z}^2) E_x - \gamma_{\text{I}z}\gamma_{\text{I}x} E_z = 0 \tag{26}$$

$$-\gamma_{\text{I}z}\gamma_{\text{I}x} E_x + (k^2 n_2^2 + \gamma_{\text{I}x}^2) E_z = 0. \tag{27}$$

For the above two equations to be compatible, we need the following condition:

$$\frac{k^2 n_1^2 + \gamma_{\text{I}z}^2}{\gamma_{\text{I}z}\gamma_{\text{I}x}} = \frac{\gamma_{\text{I}z}\gamma_{\text{I}x}}{k^2 n_2^2 + \gamma_{\text{I}x}^2}. \tag{28}$$

Substituting $\gamma_{Ix} = \gamma_I \cos \alpha$ and $\gamma_{Iz} = \gamma_I \sin \alpha$ into the above equation yields

$$\gamma_I^2 = \frac{-k^2 n_1^2 n_2^2}{n_1^2 \cos^2 \alpha + n_2^2 \sin^2 \alpha}. \tag{29}$$

We note that

$$\gamma_I^2 = -k^2 n_1^2 \qquad \text{when } \alpha = \frac{\pi}{2}. \tag{30}$$

Subtracting (29) from (25),

$$\gamma_{II}^2 - \gamma_I^2 = \frac{-k^2 n_2^2 (n_2^2 - n_1^2) \sin^2 \alpha}{n_1^2 \cos^2 \alpha + n_2^2 \sin^2 \alpha}. \tag{31}$$

Since $n_1 \approx n_2 \approx 1$ and $\gamma_I \approx \gamma_{II} \approx jk$,

$$\gamma_{II} - \gamma_I \approx jk(n_2 - n_1) \sin^2 \alpha. \tag{32}$$

REFERENCES

1. T. Oguchi, "Attenuation of Electromagnetic Waves Due to Rain with Distorted Raindrops," J. Radio Res. Labs. (Tokyo), Part I in *7*, No. 33 (September 1960), pp. 467–485; Part II in *11*, No. 53 (January 1964), pp. 19–44.
2. D. T. Thomas, "Cross Polarization Discrimination in Microwave Radio Transmission Due to Rain," Radio Science, *6*, October 1971, pp. 833–839.
3. D. C. Hogg, "Depolarization of Microwaves in Transmission Through Rain," AGARD Conference, Telecommunications Aspects on Frequencies Between 10 and 100 GHz, September 1972, Preprint CPP-107, p. 6–1.
4. P. A. Watson and M. Arbabi, "Rainfall Cross Polarization at Microwave Frequencies," Proc. IEE, *120*, April 1973, pp. 413–418.
5. R. A. Semplak, "Effect of Oblate Raindrops on Attenuation at 30.9 GHz," Radio Science, *5*, March 1970, pp. 559–564.
6. R. A. Semplak, "The Effect of Rain on Circular Polarization at 18 GHz," B.S.T.J., *52*, No. 6 (July–August 1973), pp. 1029–1031.
7. W. T. Barnett, "Some Experimental Results on 18 GHz Propagation," Conference Record of the 1972 National Telecommunications Conference, Houston, Texas; IEEE Publication 72 CHO 601-5-NTC, pp. 10E-1 to 10E-4.
8. W. T. Barnett, "Deterioration of Cross-Polarization Discrimination During Rain and Multipath Fading at 4 GHz," Conference Record of the 1974 International Conference on Communications, Minneapolis, Minn., IEEE Publication 74 CHO 859-9-CSCB, pp. 12D-1 to 12D-4.
9. M. J. Saunders, "Cross Polarization at 18 and 30 GHz Due to Rain," IEEE Transactions on Antennas and Propagation, *AP-19*, March 1971, pp. 273–277.
10. J. A. Morrison, M.-J. Cross, and T. S. Chu, "Rain-Induced Differential Attenuation and Differential Phase Shift at Microwave Frequencies," B.S.T.J., *52*, No. 4 (April 1973), pp. 599–604.
11. J. A. Morrison and T. S. Chu, "Perturbation Calculations of Rain-Induced Differential Attenuation and Differential Phase Shift at Microwave Frequencies," B.S.T.J., *52*, No. 10 (December 1973), pp. 1907–1913.
12. J. A. Morrison and M.-J. Cross, "Scattering of a Plane Electromagnetic Wave by Axisymmetric Raindrops," B.S.T.J., *53*, No. 6 (July–August 1974), pp. 955–1019.
13. T. Oguchi, "Attenuation and Phase Rotation of Radio Waves Due to Rain: Calculations at 19.3 and 34.8 GHz," Radio Sci., *8*, No. 1 (January 1973), pp. 31–38.
14. T. Oguchi and Y. Hosoya, "Differential Attenuation and Differential Phase Shift of Radio Waves Due to Rain: Calculations at Microwave and Millimeter Wave Regions," presented at the I.U.C.R.M. Colloquium, October 1973, Nice, France.

15. H. R. Pruppacher and R. L. Pitter, "A Semi-Empirical Determination of the Shape of Cloud and Rain Drops," Journal of the Atmospheric Sciences, *28*, January 1971, pp. 86–94.
16. H. C. Van de Hulst, *Light Scattering by Small Particles*, New York: John Wiley, 1957.
17. P. S. Ray, "Broadband Complex Refractive Indices of Ice and Water," Appl. Opt., *11*, August 1972, pp. 1836–1844.
18. D. E. Setzer, "Computed Transmission Through Rain of Microwave and Visible Frequencies," B.S.T.J., *49*, No. 8 (October 1970), pp. 1873–1892.
19. O. E. Delange, A. F. Dietrich, and D. C. Hogg, "An Experiment on Propagation of 60-GHz Waves Through Rain," to be published in B.S.T.J., January 1975.
20. P. A. Watson and M. Arbabi, "Cross Polarization Isolation and Discrimination," Elec. Lett., *9*, November 1, 1973, pp. 516–517.
21. V. H. Rumsey et al., "Techniques for Handling Elliptically Polarized Waves with Special Reference to Antennas," Proc. IRE, *39*, May 1951, pp. 533–552.
22. S. H. Lin, private communication.
23. G. C. McCormick and A. Hendry, "Polarization Properties of Transmission through Precipitation over a Communication Link," presented at the I.U.C.R.M. Colloquium, October 1973, Nice, France.
24. R. A. Semplak, "Simultaneous Measurements of Depolarization by Rain Using Linear and Circular Polarizations at 18 GHz," B.S.T.J., *53*, No. 2 (February 1974), pp. 400–404.
25. R. A. Semplak, "Measurements of Rain-Induced Polarization Rotation at 30 GHz," Radio Science, *9*, April 1974, pp. 425–429.
26. P. A. Watson and M. Arbabi, "Rainfall Cross-Polarization, Comparison of Theory and Measurement," presented at the I.U.C.R.M. Colloquium, October 1973, Nice, France.
27. B. G. Evans and P. T. Thompson, "Cross-Polarization due to Precipitation at 11.6 GHz," presented at the I.U.C.R.M. Colloquium, October 1973, Nice, France.
28. H. Yamamoto et al., "Experimental Considerations on 20 GHz High-Speed Digital Radio-Relay System," Conference Record of 1973 IEEE International Conference on Communications, pp. 28–37 to 28–42.
29. C. W. Bostian et al., "Millimeter Wave Rain Depolarization: Some Recent 17.65 GHz Measurements," 1973 G-AP International Symposium Digest, pp. 289–292.
30. B. G. Evans and J. Troughton, "Calculation of Cross-Polarization Due to Precipitation," IEE Conference on Propagation of Radio Waves at Frequencies above 10 GHz, April 1973, pp. 162–171.